THERMODYNAMIC MODELING OF PYROMETALLURGICAL OXIDE SYSTEMS CONTAINING Mn OXIDES

Youn-Bae Kang
École Polytechnique, Canada

In-Ho Jung
McGill University, Canada

ABSTRACT

Thermodynamic modeling for the CaO-MgO-Al_2O_3-SiO_2-FeO_x-CrO_x-TiO_x-MnO_x oxide system at oxygen partial pressures from metal saturation to 1 bar has been conducted in order to understand Mn oxide behavior in various metallurgical processes. The thermodynamic properties of molten slag were described by the Modified Quasichemical Model considering the silicate network structure. The complex solid solutions such as spinel, olivine, pseudobrookite, etc. were modeled in the framework of the Compound Energy Formalism considering their crystal structures. The model with optimized model parameters can calculate the phase diagrams of any sections of binary, ternary and multicomponent systems with various oxygen partial pressures. By coupling with the available thermodynamic databases for gas and alloys, unexplored complex phase equilibria and chemical reactions between gas/slag/refractory/inclusion/alloys can be easily calculated for various metallurgical processes. The successful applications of thermodynamic calculations to inclusion controls for Mn/Si/Ti containing steel, chemical reactions between gas/slag/liquid Fe-Mn alloy for Fe-Mn production, etc. demonstrate the applicability of the thermodynamic modeling to metallurgical processes.

INTRODUCTION

In recent years, thermodynamic modeling has been actively pursued apace with the improvement of computational techniques and software. Based on a proper thermodynamic model for every phase of a given system, all available thermodynamic and phase equilibrium data for a system are critically and simultaneously evaluated in order to obtain one self-consistent set of model equations for the Gibbs energies which best reproduces the data for all phases as functions of temperature and composition. In this way, the thermodynamic databases are developed. The databases are then used, along with Gibbs energy minimization software, to calculate multicomponent phase equilibria of importance for various applications. This technique has come to be known as thermodynamic *optimization or modeling*. The models and optimized model parameters for low-order (binary and ternary) sub-systems can be used to provide good estimates for unexplored higher-order system where data are lacking.

Over the last several years, accurate thermodynamic modeling for various Mn oxide systems of CaO-MgO-Al_2O_3-SiO_2-FeO_x-CrO_x-TiO_x-MnO_x has been conducted by the authors with the view to facilitate the simulations of industrial metallurgical processes containing Mn oxides.

In the present study, the progress of new thermodynamic modeling of various Mn oxide systems will be summarized and then the versatility and accuracy of the developed thermodynamic databases will be demonstrated by the applications to inclusion engineering and gas/slag/inclusion/metal reactions in steelmaking and Fe-Mn production.

THERMODYNAMIC MODELING

The aim of the present study is the extension of the current FACT oxide database [1] toward Mn oxide systems. The FACT databases for multicomponent oxide, salt, alloy and aqueous solutions have been developed by critical evaluation/optimization of all available thermodynamic data over the last 25 years. The databases contain over 4400 compounds and 120 non-ideal multicomponent solution phases.

The FACT oxide solution database contains critically evaluated thermodynamic data for the molten slag phase and for many extensive oxide solid solutions containing the following components: Al_2O_3, As_2O_3, B_2O_3 , CaO, CoO, CrO, Cr_2O_3, Cu_2O, FeO, Fe_2O_3, GeO_2, K_2O, Na_2O, MgO, MnO, NiO, PbO, SiO_2, SnO, TiO_2, Ti_2O_3, ZnO, ZrO_2. Not all possible combinations of these components have been critically evaluated. Generally, the critical assessment and optimization of model parameters have been done for certain subsystems of this 23-component system which are of particular importance for various applications in materials science, metallurgy, ceramics, geology, cement, combustion, energy, glass technology, corrosion, etc.

In the present study, Mn oxides of various valence states such as Mn^{2+}, Mn^{3+} and Mn^{4+} were taken into account in thermodynamic modeling for the extension of current FACT oxide database. The major systems achieved in the present study include: Mn-O (MnO-Mn_2O_3-MnO_2), Mn-Fe-O (MnO-Mn_2O_3-FeO-Fe_2O_3), Mn-Cr-O (MnO-Mn_2O_3-CrO-Cr_2O_3), Mn-Si-O (MnO-Mn_2O_3-SiO_2), Mn-Fe-Si-O (MnO-Mn_2O_3-FeO-Fe_2O_3-SiO_2), CaO-MnO-Al_2O_3-SiO_2, MnO-Ti_2O_3-TiO_2-SiO_2, etc. Numerous solid compounds, solid solutions and liquid phase were thermodynamically modeled in the temperature range from 25°C to above liquidus and at PO_2 from metallic saturation to over 100 bar.

The molten slag phase is modeled by the Modified Quasichemical Model [2, 3, 4] in which short-range-ordering of molten silicate is well taken into account. In the molten slag, various valence states of oxides of transition metals such as Fe (Fe^{2+}, Fe^{3+}), Mn (Mn^{2+},

Mn^{3+}) and Ti (T^{3+}, Ti^{4+}) are also considered. Ceramic solid solutions are mainly modeled in the framework of the Compound Energy Formalism [5], taking into account the crystal structure and physical nature of each solid solution. For example, the model for spinel (cubic and tetragonal) describes the distribution of cations and vacancies over tetrahedral (T) and octahedral (O) sites: $(Al^{3+}, Co^{2+}, Co^{3+}, Cr^{2+}, Cr^{3+}, Fe^{2+}, Fe^{3+}, Mg^{2+}, Ni^{2+}, Zn^{2+}, Mn^{2+}, Mn^{3+})^{T}[Al^{3+}, Co^{2+}, Co^{3+}, Cr^{3+}, Fe^{2+}, Fe^{3+}, Mg^{2+}, Ni^{2+}, Zn^{2+}, Mn^{2+}, Mn^{3+}, Mn^{4+}, Va]_2^{O}O_4$. Olivine solution is modeled by considering two octahedral sites: $[Ca^{2+}, Co^{2+}, Fe^{2+}, Mg^{2+}, Mn^{2+}, Ni^{2+}, Zn^{2+}]^{M2}(Ca^{2+}, Co^{2+}, Fe^{2+}, Mg^{2+}, Mn^{2+}, Ni^{2+}, Zn^{2+})^{M1}SiO_4$.

In the present study, we combined the newly optimized model parameters with current FACT oxide database. Then, various phase diagram and thermodynamic calculations for the applications to steelmaking and Fe-Mn production were performed along with other FACT databases such as FACT liquid steel database [6].

RESULTS OF THERMODYNAMIC MODELING OF MnO CONTAINING SYSTEMS

In the thermodynamic model, all kinds of available thermodynamic data such as solid/liquid/gas phase equilibria, phase diagrams, calorimetric data, electrochemical data, vapour pressures, activities of components, even crystal structures, etc. are collected and critically evaluated and simultaneously optimized. In the following, parts of the thermodynamic modeling results are presented.

Figure 1 shows the optimized phase diagram of the Mn-O system. In general, the phase diagram is similar to Fe-O system. As can be seen in the diagram, manganosite (MnO) and β-Mn_3O_4 spinel can be deviated considerably from their stoichiometric compositions. MnO and Mn_2O_3 are considered for molten slag components. The variation of oxygen partial pressure profiles in all solid phases and liquid phase are accurately modeled.

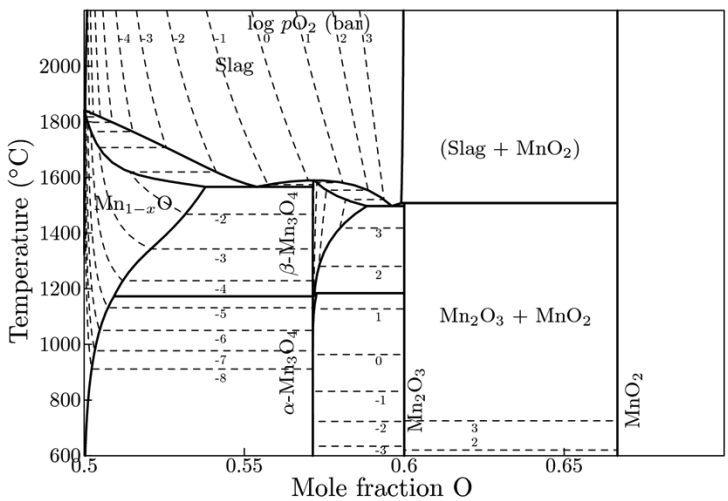

Figure 1: Optimized phase diagram of the Mn-O system

Figures 2 and 3 present the phase diagrams of the Mn-Si-O system at reducing condition (metallic saturation) and oxidizing condition (air), respectively. As can be seen in the figures, the phase assemblages are completely changed with oxygen partial pressure.

For example, solid Mn_2SiO_4 and $MnSiO_3$ phases become unstable with increase of oxygen partial pressures and solid spinel phase appears instead of MnO phase.

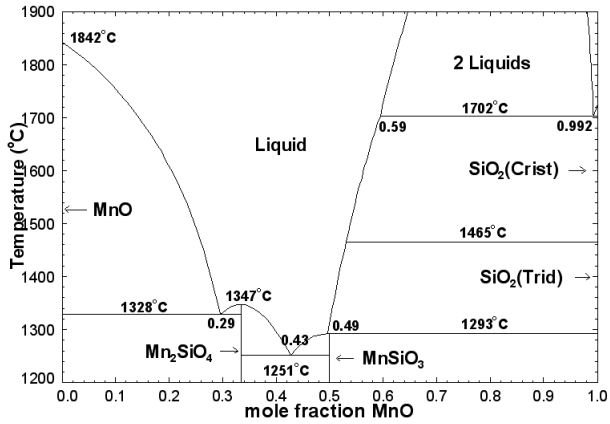

Figure 2: Optimized phase diagram for the Mn-Si-O system at metallic saturation [7]

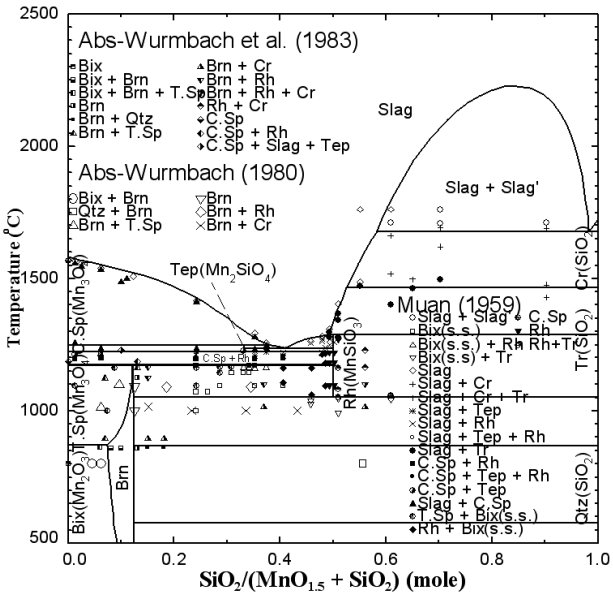

Figure 3: Optimized phase diagram for the Mn-Si-O system in air along with experimental data [8, 9, 10]

The optimized phase diagrams of the Fe-Mn-O system at metallic saturation and in air are presented in Figure 4. Mangano-wustite phase (MW) is in equilibration with molten slag at metallic saturation, On the other hand, cubic spinel (C.Sp) phase is in equilibration with molten slag in air. Corundum solid solution and Bixbyte solid solution are also stable at subsolidus temperature in air.

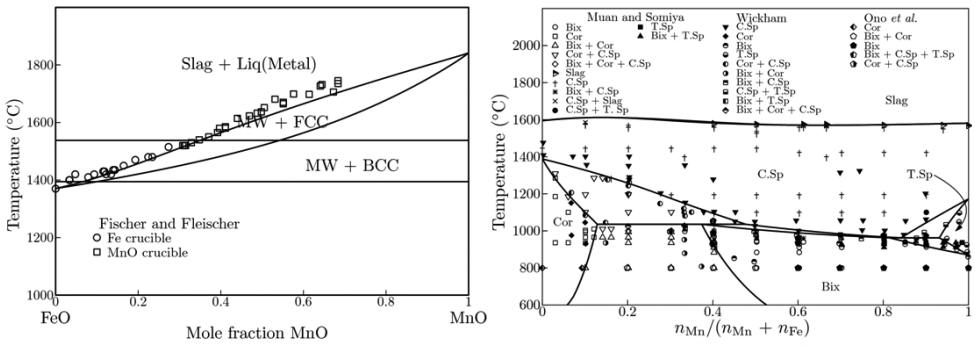

(a) (b)

Figure 4: Optimized phase diagram of the Fe-Mn-O system (a) at metallic saturation and (b) in air along with experimental data [11, 12, 13]

Figure 5 shows the optimized phase diagram of the Mn-Cr-O system in air and at log pO_2 = -8.0. The phase assemblages are also varied considerably with oxygen partial pressures. Recently this system becomes important for slag chemistry and inclusion control of high Mn stainless steel. In addition, this is one of the key oxide systems to understand the oxidation of special stainless steel for SOFC interconnect applications.

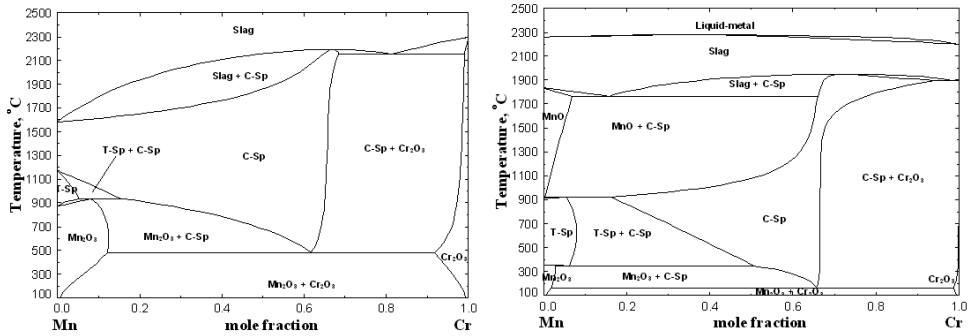

(a) (b)

Figure 5: Calculated phase diagram of the Mn-Cr-O system [14a, b] at various partial pressures (a) air and (b) log P_{02} = -8.0

Figure 6 shows the optimized liquid projection for the Fe-Mn-Si-O system at metallic Fe saturation and in air. As can be seen in the diagram, the primary crystalline phase can be completely changed depending on the oxygen partial pressures. In the case of the Fe saturation, Fe_2SiO_4-Mn_2SiO_4 olivine and mangano-wustite have large primary crystalline areas. While, Fe_3O_4-Mn_3O_4 spinel phase covers large primary area in oxidizing condition. Iso-activity lines of FeO and MnO against their solid standard states are calculated for the Fe-Mn-Si-O system at metallic Fe saturation and presented in Figure 7. The calculated lines are in good agreement with experimental data [15, 16].

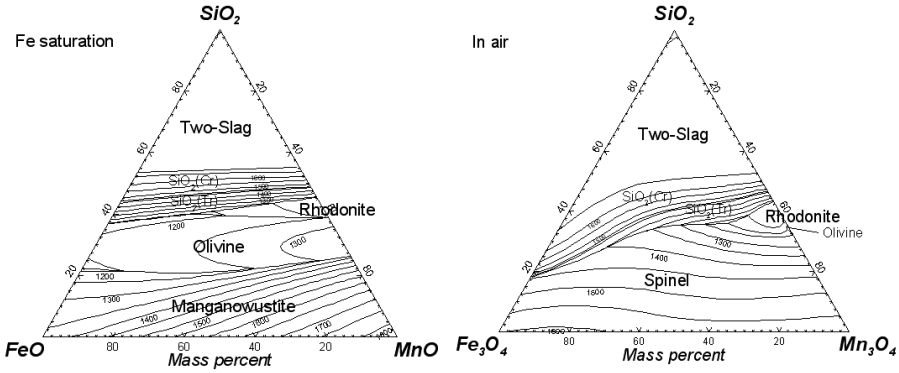

Figure 6: Optimized phase diagram of the Fe-Mn-Si-O system (a) at metallic saturation and (b) in air

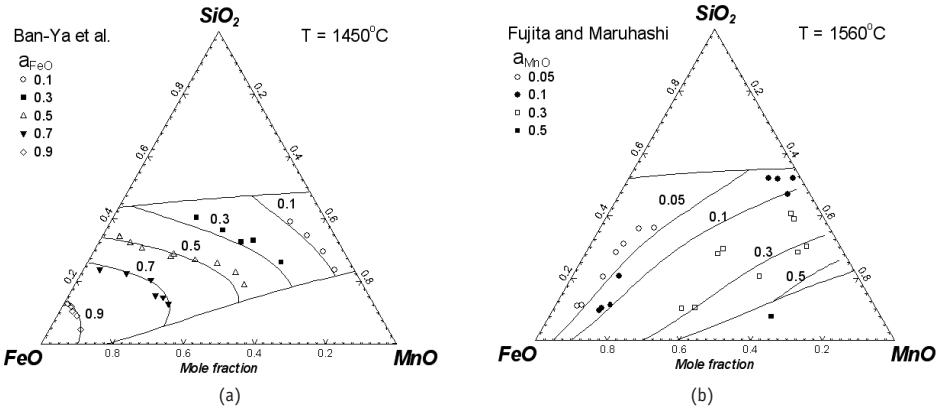

Figure 7: Calculated iso-activity lines of (a) solid FeO at 1450°C and (b) solid MnO at 1560°C in the Fe-Mn-Si-O system at metallic Fe saturation along with experimental data [15, 16]

Recently we have performed intensive thermodynamic modeling study data [17, 19] on the CaO-MnO-Al_2O_3-SiO_2 system for the applications to inclusion engineering for Mn/Si deoxidized steels. The MnO-Al_2O_3 system was reoptimized with correct Gibbs energy of $MnAl_2O_4$ galaxite. We found the tabulated Gibbs energy by Barin [20] is about 40 kJ/mol off from the experimental data. Figure 8 shows the calculated liquidus projection of the MnO-Al_2O_3-SiO_2 system at metallic saturation. Iso-activity lines of SiO_2 and Al_2O_3 at 1600°C are calculated and presented in Figure 9. Both phase diagrams and activity data were taken into account in the thermodynamic modeling of the system.

Calculated phase diagrams of the MnO-SiO_2-Ti_2O_3-TiO_2 system [21, 22] at various oxygen partial pressures are presented in Figure 10. Under these relatively reducing oxygen partial pressures, Mn^{3+} concentration in slags and solid phases are negligible, however, valences of Ti in oxides (Ti^{3+} and Ti^{4+}) are greatly affected by the oxygen partial pressure, which is sometime overlooked in the experiments. Consequently, phase diagrams look very different depending on pO_2.

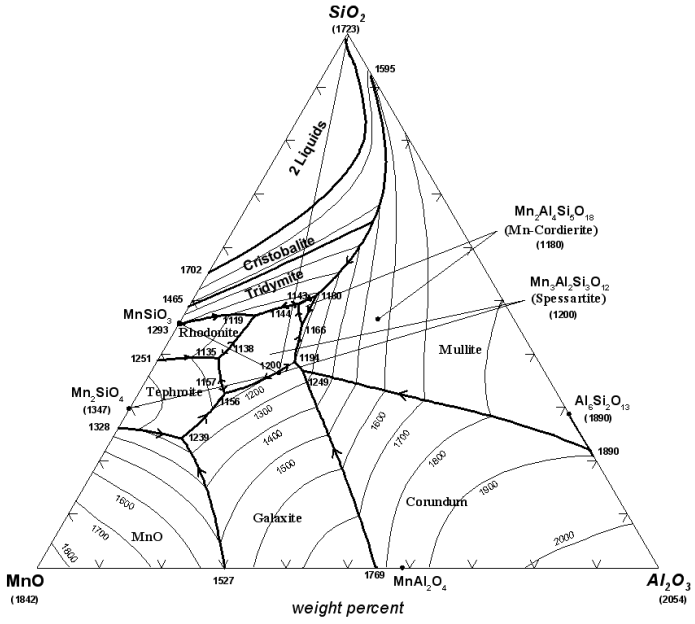

Figure 8: Calculated liquidus projection of MnO-Al_2O_3-SiO_2 system [17]

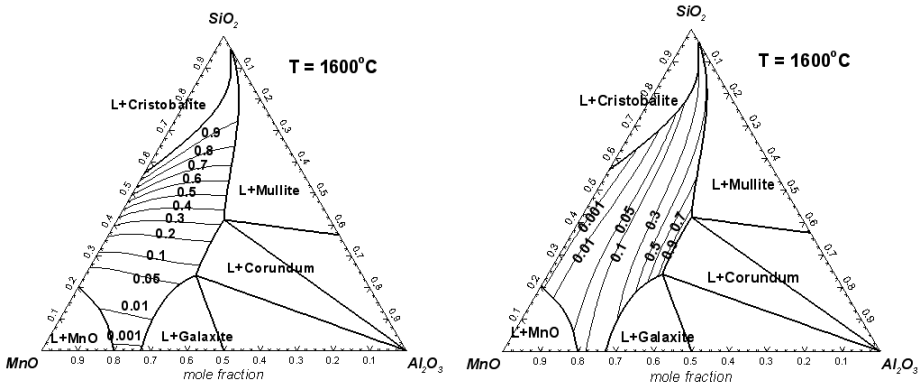

Figure 9: Calculated activity of (a) solid SiO_2 and (b) Al_2O_3 in the MnO-Al_2O_3-SiO_2 system at 1600ºC [17]

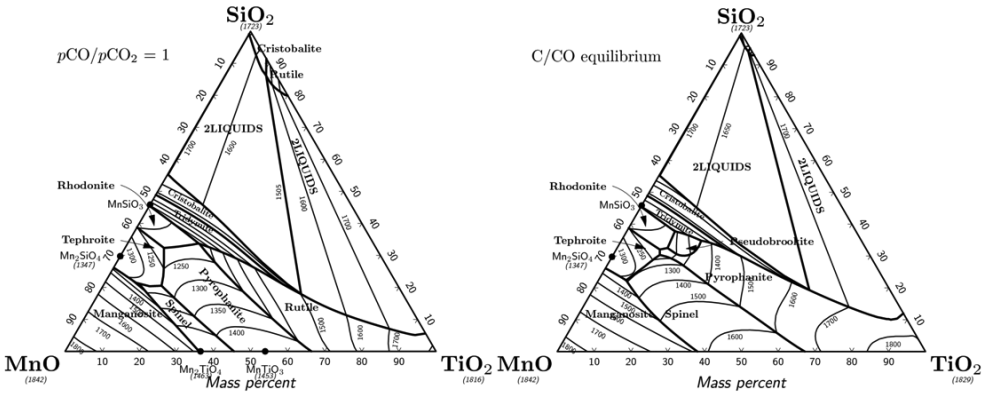

Figure 10: Calculated liquidus projection in the MnO-SiO_2-TiO_2-Ti_2O_3 system [22]

APPLICATIONS TO PYROMETALLURGICAL PROCESS

Inclusion Controls in Mn/Si Deoxidation Process

Control of inclusions is important in the production of high quality steels. Inclusions in Mn/Si deoxidized steel are mainly composed of MnO and SiO_2. However, impurities such as aluminum in ferro-alloy may be introduced in molten steel and react with oxygen so that most typical inclusions in Mn/Si deoxidized steel belong to the MnO-SiO_2-Al_2O_3 system. In case of Mn/Si deoxidized steel such as tire cord and INVAR steels, the minimization of solid inclusion and obtaining liquid inclusions even at wire-making and rolling temperatures of about 1100°C to 1200°C are important. In order to control inclusions in Mn/Si deoxidized steel, the interactions between Mn/Si deoxidized steel and the MnO-SiO_2-Al_2O_3 inclusion were calculated using the thermodynamic database.

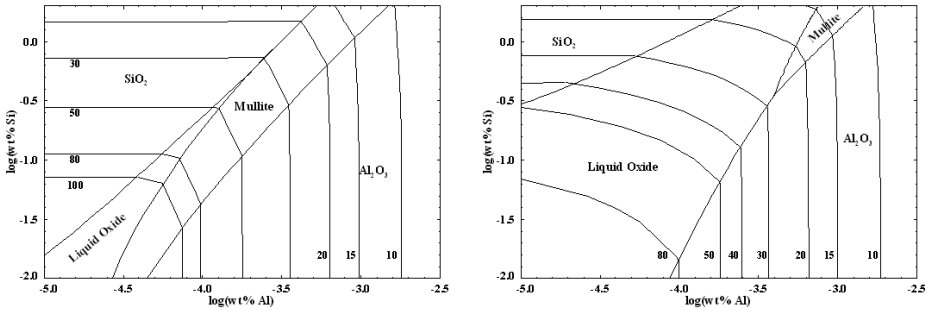

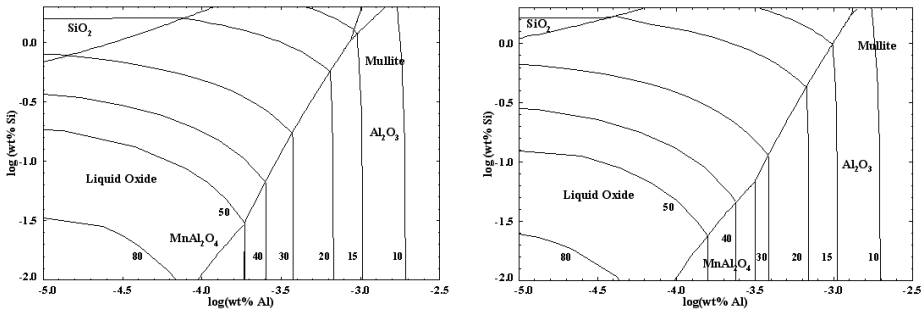

Figure 11: Calculated inclusion stability diagrams in the Fe-Mn-Si-Al-O system at 1550ºC for (a) mass% Mn = 0, (b) mass% Mn = 0.5, (c) mass% Mn = 1.0 and (d) mass% Mn = 1.5. Numbers adjacent to each line represent equilibrium oxygen contents (in ppm) in liquid steel [23].

Figure 11 shows the calculated inclusion stability diagram in the Fe-Mn-Si-Al-O system at 1550°C [23]. Without Mn, inclusions of SiO_2-Al_2O_3 system can form in steel and the stability area of liquid oxide is quite small compared with those of solid SiO_2, mullite and Al_2O_3. The stability area of liquid oxide phase of MnO-SiO_2-Al_2O_3 increases with the increase of Mn content in steel. On the other hand, the stability areas of mullite and SiO_2 become smaller. $MnAl_2O_4$ stability area appears with increase of Mn concentration.

In the case of steel containing Mn = 1.5 wt% and Si = 1wt%, for example, liquid oxide inclusion can be obtained at [Al] < 10 ppm. If [Al] > 10 ppm, solid Al_2O_3 inclusion can be generated in liquid steel. Thus, the inclusion stability diagram can provide valuable information regarding inclusion formation at the given molten steel composition.

Evolution of Inclusions

Recently beneficial effects of inclusions on steel properties have been recognized, and the technology to use these inclusions is termed as *oxide metallurgy*. For example, inclusions of Mn-Si-O-S system have been known as intragranular nucleation sites for acicular ferrite, resulting in a reduced grain size and consequently improved physical properties of steel. Recently, inclusions formed in (Mn-Si-Ti)-deoxidized steels have attracted much attention because so-called *Mn-depleted zone* can be well developed around these inclusions after proper thermal treatments. The Mn-depleted zone plays a key role in the acicular ferrite formation.

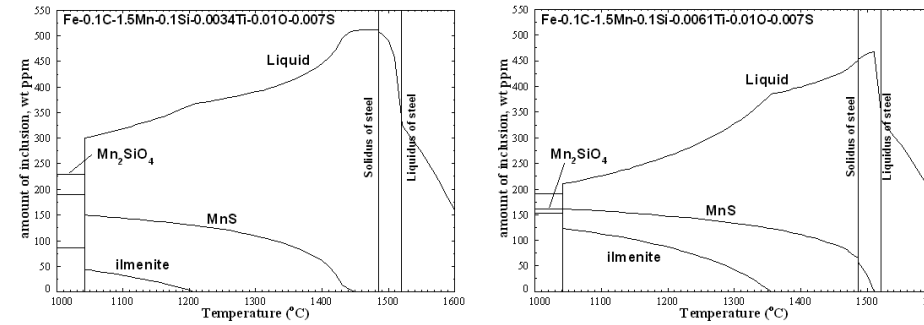

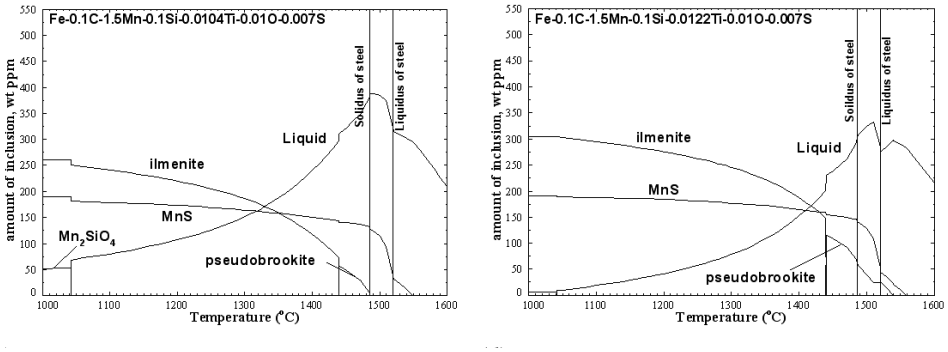

Figure 12: Evolutions of inclusions in Mn/Si/Ti steel during solidification, calculated from thermodynamic databases. (a) 34ppm Ti, (b) 61ppm Ti, (c) 104ppm Ti and (d) 122ppm Ti [24]

The evolutions of inclusions in the Mn/Si/Ti steels (Fe-0.1C-1.5Mn-0.1Si-0.01O-0.007S-Ti) were calculated and presented in Figure 12 [27]. As seen in the figure, the portion of liquid phase in the entire inclusion decreases with the increase of Ti content. In the case of Ti = 104 and 122 ppm, the amount of liquid becomes less than 20 mass percent at 1200°C. In the cooling process, ilmenite phase becomes dominant with the increase of Ti content.

According to the thermodynamic calculations, MnS can be precipitated from liquid inclusion phase when Ti contents are 34 and 61 ppm. On the contrary, when Ti contents are 104 and 122 ppm MnS precipitates during steel solidification. That is, in the case of the MnS precipitation from liquid inclusion ((a) and (b)), MnS can be precipitated inside of oxide inclusion. When MnS precipitates mainly during steel solidification ((c) and (d)), MnS can be precipitated as separate phase or on the surface of oxide inclusion. This precipitation behavior changes the morphology of inclusions.

Extensive experimental studies to understand the evolution of inclusion during the solidification of various steel containing Mn-Si-Ti-Al-Mg have been conducted by Prof. H.-G. Lee and his colleagues [25, 26, 27, 28, 29, 30, 31] (GIFT, POSTECH in S. Korea), in strong collaboration with the present authors for the thermodynamic analysis.

High Mn-Fe Alloy Production

Mn-Fe alloys are normally produced using carbothermic reduction process. Thus, considerable amount of carbon can be contained in Mn-Fe alloys prior to final refining. During refining process of Mn-Fe alloys, CaO-MnO-SiO_2-Al_2O_3 slags are in equilibration with liquid Mn-Fe alloys and the distribution of Mn between the slags and Mn-Fe alloys is important in order to increase the yield of Mn.

Figure 13 shows the calculated slag composition in the equilibration with liquid Mn-11%Fe-Si-C alloy at 1500°C [22]. In the figure, heavy lines represent liquidus lines of specified solid phases at 1500°C. The ratio of CaO/Al_2O_3 of the slag is fixed to be 1.5. Ding and Olsen [32] equilibrated CO gas/ liquid slag/ liquid Mn-11%Fe-Si-C at 1500°C and analyzed the equilibrium slag compositions. The calculated slag compositions represented as dotted line in figure are in good agreement with experimental results of Ding and Olsen. We also have tested many other conditions and found excellent agreement with experimental data. This sample calculation shows the applicability of the present thermodynamic modeling to Mn-Fe production.

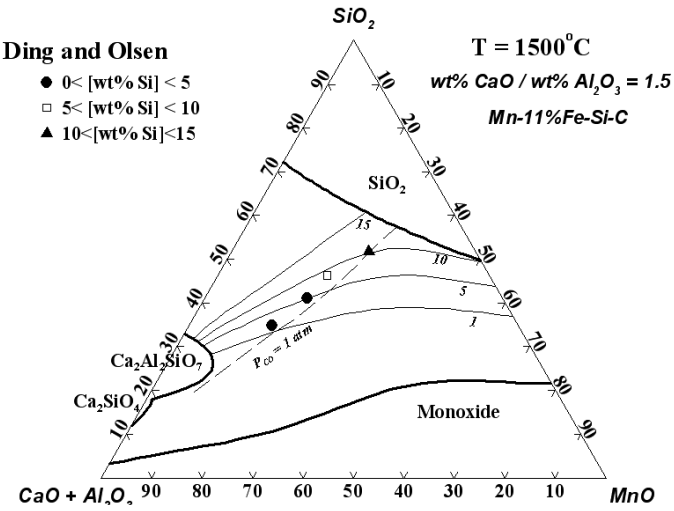

Figure 13: Calculated composition of the CaO-MnO-SiO_2-Al_2O_3 liquid slag with CaO/Al_2O_3 ratio of 1.5 in equilibrium with Mn-11wt%Fe-Si-C alloys at 1550ºC [19]

SUMMARY

Thermodynamic modeling for the MnO oxide containing system, CaO-MgO-Al_2O_3-SiO_2-FeO_x-CrO_x-TiO_x-MnO_x at oxygen partial pressures from metal saturation to 1 bar has been conducted in order to understand Mn oxide behavior in various metallurgical process conditions. The optimization results are in good agreement with all reliable experimental data. The applicability and accuracy of new database have been tested for various metallurgical examples with great success. The optimized model parameters are combined with current FACT database and available for the thermodynamic calculations for the various metallurgical system containing Mn oxides. Further extension of the thermodynamic modeling of Mn oxides is being performed.

REFERENCES

FactSage. (2002). Ecole Polytechnique, Montréal, http://www.factsage.com. [1]

Pelton, A. D. & Blander, M. (1986). *Thermodynamic Analysis of Ordered Liquid Solutions by a Modified Quasi-Chemical Approach.* Application to Silicate Slags, Metall. Trans. B, 17B, pp. 805-815. [2]

Pelton, A. D., Decterov, S. A., Eriksson, G., Robelin, C. & Dessureault, Y. (2000). *The Modified Quasichemical Model. I - Binary Solutions, Metall.* Mater. Trans. B, Vol. 31B, pp. 651-659. [3]

Pelton, A. D. & Chartrand, P. (2001). *The Modified Quasichemical Model. II – Multi-component Solutions, Metall.* Mater. Trans. A, Vol. 32A, pp. 1355-1360. [4]

Hillert, M., Jansson, B. & Sundman, B. (1988). Application of the Compound-Energy Model to Oxide Systems, Z. Metallkd., Vol. 79, No. 2, pp. 81-87. [5]

Jung, I.-H., Decterov, S. A. & Pelton, A. D. (2004). *A Thermodynamic Model for Deoxidation Equilibria in Steel, Metall.* Mater. Trans. B, Vol. 35B, pp. 493-507. [6]

Eriksson, G., Wu, P., Blander, M. & Pelton, A. D. (1994). *Critical Evaluation and Optimisation of the Thermodynamic Properties and Phase Diagrams of the MnO-SiO_2 and CaO-SiO_2 Systems.* Can, Metall. Q., Vol. 33, No. 1, pp. 13-21. [7]

Abs-Wurmbach, I. (1980). *Miscibility and Compatibility of Braunite, $Mn^{2+}Mn^{3+}6\ O_8/SiO_4$, in the System Mn-Si-O at 1 atm in Air.* Contrib. Mineral. Petrol., 71, pp. 393–399. [8]

Abs-Wurmbach, I. Peters, T., Langer, K. & Schreyer, W. (1983). *Phase Relations in the System Mn-Si-O: an Experimental and Petrological Study.* Neues Jahrbuch Miner. Abh. 146, pp. 258–279. [9]

Muan, A. (1959). *Phase Equilibria in the System Manganese Oxide – SiO_2 in Air.* Amer. J. Sci. 275, pp. 297-315. [10]

Fischer, W. & Fleisher, H. (1961). *Die Manganverteilung zwischer Eisenschmelzen und Eisen(II)-oxydschlacken im MnO-Tiegel bei 1520 bis 1770°C.* Arch. Eisenh¨uttenwesen 32, pp. 1–10. [11]

Wickham, D. (1969). *The Chemical Composition of Spinels in the System Fe_3O_4-Mn_3O_4.* Arch. Eisenhüuttenwes 40, pp. 395–399. [12]

Ono, K., Ueda, T., Ozaki, T., Ueda, Y., Yamaguchi, A. & Moriyama, J. (1971). *Thermodynamic Study of the Iron-Manganese-Oxygen System.* Nippon Kinzoku Gakkaishi 35, pp. 757–763. [13]

Jung, I.-H. (2006). *Critical Evaluation and Thermodynamic Modeling of the Mn-Cr-O System for the Oxidation of SOFCInterconnect.* Solid State Ionics, Vol. 177, No. 7-8, pp. 765-777. [14a]

Muan, A. & Somiya, S. (1962). *The System Iron Oxide - Manganese Oxide in Air.* Amer. J. Sci. 260, pp. 230–240. [14b]

Ban-Ya S, Hino M. & Yuge N. (1985). *Activity of the Constituents in FetO-SiO_2-MnO Slags in Equilibrium with Solid Iron.* Tetsu-to-Hagane, Vol. 71, pp. 853-860. [15]

Fujita H. & Maruhashi S. (1970). *Equilibrium between FeO-MnO-SiO_2 Slags and Molten Iron.* Tetsu-to-Hagane, Vol. 56, pp. 830-851. [16]

Jung, I.-H., Kang, Y. -B., Degterov, S. A. & Pelton, A. D. (2004). *Thermodynamic Evaluation and Optimization of the MnO-Al_2O_3 and MnO-Al_2O_3-SiO_2 Systems and Applications to Inclusion Engineering.* Metall. Mater. Trans. B, Vol. 35B, pp. 259-268. [17]

Kang, Y.-B., Jung, I.-H., Degterov, S.A., Pelton, A.D. & Lee, H.-G. (2004). *Thermodynamic Evaluation and Optimization of the CaO-MnO-SiO_2 and CaO-MnO-Al_2O_3 Systems.* ISIJ Inter. Vol. 44, No. 6, pp. 965-974. [18]

Kang, Y.-B., Jung, I.-H., Degterov, S. A., Pelton, A. D. & Lee, H.-G. (2004). *Phase Equilibria and Thermodynamic Properties of the CaO-MnO-Al_2O_3-SiO_2 System by Critical Evaluation, Modeling and Experiment.* ISIJ Inter. Vol. 44, No. 6, pp. 975-983. [19]

Barin, I. (1989). *Thermodynamic Data for Pure Substances.* VCH, Weinheim, Germany. [20]

Kang, Y.-B., Jung, I.-H. & Lee, H.-G. (2006). *Critical Thermodynamic Evaluation and Optimization of the MnO-"TiO_2"-"Ti_2O_3" System.* Calphad, Vol. 30(3), pp. 235-247. [21]

Kang, Y.-B., Jung, I.-H. & Lee, H.-G. (2006). *Critical Thermodynamic Evaluation and Optimization of the MnO-SiO_2-"TiO_2"-"Ti_2O_3" System.* Calphad, Vol. 30(3), pp. 226-234. [22]

Kang, Y.-B. & Lee, H.-G. (2004). *Inclusions Chemistry for Mn/Si Deoxidized Steels: Thermodynamic Predictions and Experimental Confirmations.* ISIT Inter. Vol. 44, pp. 1006-1015. [23]

Kang, Y.-B., Chang, C.-H., Park, S.-C., Kim, H.-S., Jung I.-H. & Lee, H.-G. (2004). *Inclusion Control in Steels containing Si, Mn, Ti, Mg and/or Al: Thermodynamic Prediction and Experimental Confirmation.* Metal Separation Technology III – Symp. in Honour of Prof. Lauri E. Holappa of the Helsinki University of Technology, Laboratory of Metallurgy, Helsinky University of Technology, Helsinky, Finland, pp. 325-334. [24]

Kim, H.-S., Lee, H.-G. & Jung, W.-G. (2000). *Optimization of Steel Chemistry for MnS Precipitation on Oxide Inclusions in Si/Mn Deoxidized Steel.* ISIJ Int., Vol. 40, pp. S82-S86. [25]

Kim, H.-S., Lee, H.-G. & Oh, K.-S. (2000). *Precipitation Behavior of MnS on Oxide Inclusions in Si/Mn Deoxidized Steel.* Metals and Materials, Vol. 6, pp. 305-310. [26]

Kim, H.-S., Lee, H.-G. & Oh, K.-S. (2001). *MnS Precipitation in Association with Manganese Silicate Inclusions in Si/Mn Deoxidized Steel.* Metall. Mater. Trans. A, Vol. 32A, pp. 1519-1525. [27]

Kim, H.-S., Lee, H.-G. & Oh, K.-S. (2002). *Evolution of Size, Composition, and Morphology of Primary and Secondary Inclusions in Si/Mn and Si/Mn/Ti Deoxidized Steels*. ISIJ Int., Vol. 42, pp. 1404-1411. [28]

Kim, H.-S., Chang, C.-H. & Lee, H.-G. (2005). *Evolution of Inclusions and Resultant Microstructural Change with Mg Addition in Mn/Si/Ti Deoxidized Steels.* Scripta Mater., Vol. 53, pp. 1253-1258. [29]

Chang, C.-H., Jung, I.-H., Park, S.-C., Kim, H.-S. & Lee, H.-G. (2005). *Effect of Mg on the Evolution of Non-metallic Inclusions in the Mn-Si-Ti Deoxidized Steel during Solidification: Experiments and Thermodynamic Calculations.* Ironmaking and Steelmaking, Vol. 34, No. 3, pp. 251-257. [30]

Park, S.-C., Jung, I.-H., Oh, K.-S. & Lee, H.-G. (2004). *Effects of Al on the Evolution of Non-metallic Inclusions in the Mn-Si-Ti-Mg Deoxidized Steel during Solidification: Experiments and Thermodynamic Calculations*. ISIJ Inter. Vol. 44, No. 6, pp. 1016-1023. [31]

Ding, W. & Olsen, S. E. (1996). *Reactions between Multicomponent Slags and Mn-Fe-Si-C Alloys. Equilibrium and Stoichiometry.* Scand. J. Metall., 25, pp. 232-243. [32]